Contrib Mineral Petrol (1996) 125: 200–212

L.Ya. Aranovich · R.C. Newton

H_2O activity in concentrated NaCl solutions at high pressures and temperatures measured by the brucite-periclase equilibrium

Received: 1 September 1995 / Accepted: 24 March 1996

Abstract H_2O activities in concentrated NaCl solutions were measured in the ranges 600°–900° C and 2–15 kbar and at NaCl concentrations up to halite saturation by depression of the brucite ($Mg(OH)_2$) – periclase (MgO) dehydration equilibrium. Experiments were made in internally heated Ar pressure apparatus at 2 and 4.2 kbar and in 1.91-cm-diameter piston-cylinder apparatus with NaCl pressure medium at 4.2, 7, 10 and 15 kbar. Fluid compositions in equilibrium with brucite and periclase were reversed to closures of less than 2 mol% by measuring weight changes after drying of punctured Pt capsules. Brucite-periclase equilibrium in the binary system was redetermined using coarsely crystalline synthetic brucite and periclase to inhibit back-reaction in quenching. These data lead to a linear expression for the standard Gibbs free energy of the brucite dehydration reaction in the experimental temperature range: ΔG° ($\pm$120J)=73418–134.95T(K). Using this function as a baseline, the experimental dehydration points in the system $MgO-H_2O-NaCl$ lead to a simple systematic relationship of high-temperature H_2O activity in NaCl solution. At low pressure and low fluid densities near 2 kbar the H_2O activity is closely approximated by its mole fraction. At pressures of 10 kbar and greater, with fluid densities approaching those of condensed H_2O, the H_2O activity becomes nearly equal to the square of its mole fraction. Isobaric halite saturation points terminating the univariant brucite-periclase curves were determined at each experimental pressure. The five temperature-composition points in the system $NaCl-H_2O$ are in close agreement with the halite saturation curves (liquidus curves) given by existing data from differential thermal analysis to 6 kbar. Solubility of MgO in the vapor phase near halite saturation is much less than one mole percent and could not have influenced our determinations. Activity concentration relations in the experimental P-T range may be retrieved for the binary system H_2O-NaCl from our brucite-periclase data and from halite liquidus data with minor extrapolation. At two kbar, solutions closely approach an ideal gas mixture, whereas at 10 kbar and above the solutions closely approximate an ideal fused salt mixture, where the activities of H_2O and NaCl correspond to an ideal activity formulation. This profound pressure-induced change of state may be characterized by the activity (a) – concentration (X) expression: $a_{H_2O}=X_{H_2O}/(1+\alpha X_{NaCl})$, and $a_{NaCl}=(1+\alpha)^{(1+\alpha)}[X_{NaCl}/(1+\alpha X_{NaCl})]^{(1+\alpha)}$. The parameter α is determined by regression of the brucite-periclase H_2O activity data: $\alpha=\exp[A-B/\varrho_{H_2O}]-CP/T$, where A=4.226, B=2.9605, C=164.984, and P is in kbar, T is in Kelvins, and ϱ_{H_2O} is the density of H_2O at given P and T in g/cm^3. These formulas reproduce both the H_2O activity data *and* the NaCl activity data with a standard deviation of $\pm$0.010. The thermodynamic behavior of concentrated NaCl solutions at high temperature and pressure is thus much simpler than portrayed by extended Debye-Hückel theory. The low H_2O activity at high pressures in concentrated supercritical NaCl solutions (or hydrosaline melts) indicates that such solutions should be feasible as chemically active fluids capable of coexisting with solid rocks and silicate liquids (and a CO_2-rich vapor) in many processes of deep crustal and upper mantle metamorphism and metasomatism.

L.Ya. Aranovich · R.C. Newton (✉)
Department of the Geophysical Sciences,
The University of Chicago, Chicago, IL 60637, USA

Editorial responsibility: I.S.E. Carmichael

Introduction

Petrologic importance of concentrated brines

Supercritical aqueous salt solutions may equally well be regarded as concentrated brines or hydrous salt melts. Economic geologists have long invoked the action of concentrated salt solutions of igneous origin in the genesis of the porphyry ores of Cu, W, Mo and Sn (Graton 1940; Roedder 1971). Since F.G. Smith's (1948) experimental demonstration that highly concentrated chloride-sulfate-

borate solutions can coexist with H_2O-saturated granitic melts at elevated pressures, many petrologists have concluded that such salt magmas can be expelled as immiscible fluids, perhaps along with a third fluid phase, a CO_2-rich gas, in the late stage of crystallization of granitic plutons. Such complex supercritical brines may be potent agents in the formation of metallic ore deposits (e.g. Marakushev and Shapovalov 1994).

More recently, an important role of concentrated salt solutions has been suggested in a number of diverse petrologic connections, mainly from study of fluid and melt inclusions in minerals of igneous and metamorphic rocks. Lowenstern (1994) found immiscible salt-H_2O globules in glass inclusions in quartz phenocrysts from lavas of Pantelleria Island. The globules, which he termed quenched hydrosaline melts, were inferred to contain 60%–80% by weight NaCl equivalent salt content. These compositions correspond to hydrous salt magma or concentrated solutions of about 50 mol % H_2O. The coexisting peralkaline rhyolite glass had up to one weight percent of Cl. The peralkaline character of the pantellerites may be attributed in large part to a salt component in the granitic liquid which may be incompletely exsolved as a separate fluid phase during outgassing at low pressure.

Pasteris et al. (1995) deduced the action of concentrated $NaCl-CaCl_2$ brines from wall-rock alteration and fluid inclusions in the contact zone of the Duluth Gabbro, Minnesota. They documented salt concentrations up to 48 wt% and inferred that the fluids were of magmatic origin, though the concentration of salt could have been increased by a variety of secondary processes such as boiling. Sciuto and Ottonello (1995) studied fluid-rock interaction in the peridotite of Zabargad Island in the Red Sea. Their fluid inclusion analysis of metasomatic forsterite gems showed that recrystallization took place in the presence of salt solutions of equivalent NaCl concentration between 45.7 and 74.6 wt%.

Samson et al. (1995) found saline fluid inclusions with up to 49 equivalent wt% NaCl in apatite, monticellite and calcite of the Oka, Quebec, carbonatite complex. Many of the inclusions have halite daughter crystals and a variety of other mineral precipitates. They inferred that the saline fluids were exsolved from carbonatite liquids at minimum pressures of 4 to 8 kbar, and may have been instrumental in emplacement of rare earth element (REE) deposits.

Oliver (1995) and De Jong and Williams (1995) studied regional high-temperature scapolite and albite alterations of metasediments in northern Queensland, Australia. This metasomatism is associated with important Cu, Au, Pb, Ag, Zn, U and REE deposits. Both papers concluded that metasomatism and ore formation took place at mid-crustal depths by migrating hypersaline fluids. The latter study found evidence of concentrations of $NaCl+CaCl_2$ of 28–41 wt%.

Touret (1985) first reported apparently primary crystalline salt inclusions in granulites from the highest grade, Rb-depleted zone of the Bamble region, S. Norway. Fluid inclusions in some of the granulites are hypersaline brines, coexisting with dense CO_2-rich fluid inclusions of the same generation. His inference of an important fluid agency for granulite facies metamorphism consisting of near-saturated supercritical brines accompanied by an immiscible CO_2-rich phase has been reiterated in recent studies (Touret 1995). Aranovich et al. (1987) earlier argued in favor of a concentrated NaCl solution of low H_2O activity as a general mechanism in granulite metamorphism. They showed by analysis of mineral stabilities that, for some occurrences, H_2O and CO_2 activities were both low, which would be impossible if metamorphic fluids were primarily H_2O-CO_2 solutions, as some have supposed. They also noted a strong negative correlation of water activity with pressure for a number of intermediate-grade metapelites, and related it to the changes in thermodynamic mixing properties of water in the water-salt solutions, as suggested also by Shmulovich (1988).

Philippot and Selverstone (1991) found abundant concentrated brine inclusions in eclogitic veins in peridotites in the Western Alps. They identified a large variety of daughter minerals, including halite, sylvite, carbonates, anhydrite, sulfides and monazite. The hypersaline solutions were attributed to decrepitation of fluid inclusions formed earlier in eclogites of the subduction complex.

It is increasingly evident that concentrated salt solutions can play important roles in many petrogenetic processes in the deep crust and upper mantle, including regional metamorphism, metasomatism and magma formation. Quantitative discussion of these processes is currently inhibited by lack of knowledge of important properties of concentrated supercritical salt solutions at elevated temperatures and pressures. Most needed are H_2O activities, degree of ionization, solubilities of the components of silicate minerals, and partition coefficients of minor and trace elements, including heavy metals.

Previous work in the system $NaCl-H_2O$

The principal phase equilibria of $NaCl-H_2O$ have been worked out in a series of experimental studies over the past several decades. Keevil (1942) showed by measurements of NaCl solubility in coexisting steam and liquid water that $NaCl-H_2O$ is an example of a binary system having a continuous critical curve and a maximum in the three-phase coexistence curve of solid(salt)-melt-(aqueous)-vapor. Sourirajan and Kennedy (1962) experimentally achieved the maximum in the three-phase curve and measured NaCl composition of coexisting fluids to 1240 bars. These data were summarized and extended theoretically to 2000 bars by Bowers and Helgeson (1983). Their binary isobaric diagrams show a marked shrinkage of the two-phase (liquid+vapor) field with pressure, with a small two-phase envelope remaining at two kbar at very high temperatures. Above 2 kbar, $NaCl-H_2O$ fluids are everywhere supercritical. The most

recent data on the compositions of coexisting liquid and vapor in the binary are presented by Shmulovich et al. (1995).

Gunter et al. (1983) determined the effect of H_2O on the NaCl melting point (halite saturation curve) by differential thermal analysis (DTA) to 2 kbar. Koster Van Groos (1991) extended the DTA measurements to 6 kbar and compositions as H_2O-rich as $X_{H_2O}=0.724$. Sterner et al. (1992) summarized these data thermodynamically and derived activity coefficients for NaCl in the NaCl-rich portion of the binary.

Most studies of the water-rich region have confined their attention to dilute solutions, and have attempted to quantify the degree of dissociation of NaCl. Quist and Marshall (1968) measured electrical conductivity of NaCl solutions to temperatures of 800° C and pressures of 4 kbar. Their most concentrated solutions were 0.1 M. They showed that degree of dissociation depends strongly on solution density and to a lesser extent on the temperature. At two kbar, NaCl is almost completely undissociated. Franz (1982) measured H_2O activities in NaCl solutions by depression of the brucite ($Mg(OH)_2$ – periclase (MgO) – H_2O equilibrium at two kbar. He obtained three reversed brackets of the fluid composition in equilibrium with brucite and periclase at temperatures in the range 630°–650° C and NaCl concentrations as high as $X_{NaCl}=0.2$. He concluded that H_2O and undissociated NaCl ($NaCl^0$) form a nearly ideal solution. Shmulovich et al. (1982) reported experimental observations on this system at 4 kbar and two fluid compositions ($X_{NaCl}=0.16$ and 0.26), which seemed to indicate decrease in H_2O activity relative to that at 2 kbar. No systematic determinations of H_2O activity at higher pressures or more concentrated solutions have been made before the present study.

Scope of the present study

In this study we extended the brucite-periclase H_2O activity gauge to higher temperatures, pressures and to NaCl concentrations up to saturation. In order to make accurate H_2O activity calculations, it was necessary to measure the *P–T* dehydration curve of brucite accurately in the pure H_2O system, in view of the somewhat conflicting determinations of previous workers (see Fig. 1). Much of the difficulty in determination of this simply-characterized equilibrium lies in relatively fast back-reaction of fine-grained periclase to brucite during the relatively slow quenching of standard hydrothermal experimental apparatus. For this reason some workers have resorted to dynamic methods of detecting reaction progress, such as monitoring of vapor phase volume changes during brucite dehydration or rehydration taking place in slow heating and cooling cycles (Schramke et al. 1982; Philipp 1988); these studies are imprecise because of large hysteresis intervals. A more reliable brucite-periclase *P–T* curve in the $MgO-H_2O$ system is needed as a baseline for studies of equilibrium in the presence of NaCl solutions. Accurate determination of isobaric univariant temperature-fluid composition curves in the ternary system allows retrieval of the activity-concentration relation of $H_2O-NaCl$ fluids over broad ranges of pressure, temperature and NaCl concentrations. The concentration range is limited by halite saturation, where the brucite-periclase equilibria intersect isobaric $NaCl-H_2O$ liquidus curves. Accurate location of points on the NaCl saturation curve at various pressures allows us to check the DTA determinations and thermodynamic expressions of previous workers for NaCl activities at high concentration. The present data may serve as an introduction to the physical chemistry of natural deep-seated complex polyionic fluids.

Experimental methods

Starting materials

Most of the experiments of the present study were made with mechanically-mixed powders of synthetic periclase and brucite. The periclase was originally large limpid crystals of MgO prepared by an arc-fusion method by Muscle Shoals Electrochemical Co. This material was much superior to the typical commercial reagent, which is micro-crystalline. Previous investigations have encountered severe difficulties in quench back-reaction of hyperfine MgO (Johannes and Metz 1968, Franz 1982). The periclase was analyzed with the electron microprobe and found to be pure MgO, with no detectable Fe, Ni or other substituents. Brucite was prepared from this periclase by reaction with distilled H_2O at 600° C and 2 kbar for 4 days in sealed Au capsules. The result was a complete yield of coarsely-crystalline brucite. Microprobe and X-ray diffraction analysis of this material was consistent with pure $Mg(OH)_2$. A lightly-ground powder mix of the two crystalline substances was prepared in proportions such that the largest X-ray diffraction peaks were of about equal height. Numerous powder scans of the standard mix in the range 18°–44° 2θ (Cu Kα) were made to verify reproducibility of the standard pattern. One criterion of the reaction direction of an experiment was change of peak-height ratios of product to reactant.

The powder mix was sealed by welding into 1-cm lengths of 1.6-mm-diameter Pt tubing, along with weighed amounts of distilled H_2O and reagent NaCl crystals which had been previously heated at 320° C to drive off adsorbed H_2O. A typical charge consisted of about 3 mg of powder mix, 4 mg of NaCl and 2 mg of H_2O. The amount of powder mix was sufficient to absorb or relase about 0.5 mg of H_2O in a complete reaction to brucite or periclase.

Apparatus

Internally-heated argon-pressure vessels with wound Kanthal heaters were used in the experiments at 2 kbar and 4.2 kbar, and 1.91-cm-diameter piston-cylinder apparatus with NaCl pressure medium and graphite heater sleeve was used at 4.2, 7, 10 and 15 kbar. Two capsules were ordinarily placed side-by-side in each type of apparatus. After a preliminary knowledge of the phase equilibrium relations was obtained, it was usually possible to choose the compositions of the initial fluid phases of the two capsules so that a tight reversed bracket of the final fluid phase was obtained in a single experiment.

A calibrated W-3% Re versus W-25% Re thermocouple was in virtual contact with the two Pt capsules in the piston-cylinder experiments. Power input to the furnace assembly was monitored throughout a run to check for thermocouple contamination. The manufacturer (Engelhard Industries) states that the accuracy is better than ±1° C. No correction was made for the effect of pres-

sure on the thermocouple. In the gas-pressure vessel experiments, two stainless-steel-sheathed Cr-Al thermocouples were located at opposite ends of the Pt capsules, and the whole assembly was placed in a thick Cu holder to minimize thermal gradients. The Pt capsules were protected from contact with the Cu and the steel thermocouple sheaths by a packing of dried calcite powder. The thermocouples (Omega Engineering Co.) are calibrated to $\pm 0.1°$ C. The two thermocouples always read the same temperature within 2° C. Temperatures were controlled automatically and monitored with a precision millivolt-meter.

The control thermocouple (slightly the hotter of the two in most experiments) was compared with a new previously unused thermocouple after the series of experiments was concluded, to check thermocouple integrity. The old and new thermocouples were placed tip-to-tip in the heater assembly inside of the Cu holder and heated at one bar at 30° intervals from 500° to 650° C. The old thermocouple consistently read 1 to 2 degrees C higher than the new thermocouple. It is not certain if the small difference represents an actual thermal gradient inside the Cu holder or change of calibration of the old thermocouple, but in any case it is not large enough to require a correction to the recorded temperatures.

Experiments in the piston-cylinder apparatus were brought to a pressure 3 kbar lower than the final pressure and then heated. Thermal expansion of the NaCl assemblies carried the pressure to its final run value. Some bleeding of the gauge pressure during the final stages of heating was usually required to hold a nominal pressure. Under these piston-out conditions the sample pressures are believed accurate to ± 200 bars with no friction correction. However, in the 4.2 kbar experiments it was impossible to follow this procedure because the initial cold pressure was not sufficient to consolidate the pressure assemblies. Accordingly, the assemblies were first pressurized to 5 kbar, then bled to 3 kbar, and finally heated. Much bleeding was required to hold the pressure at the nominal value. Because of the anomalous pressurizing-heating procedure, some uncertainty in sample pressure must be anticipated. For this reason, some experiments at 4.2 kbar in the piston-cylinder were repeated in the gas-pressure apparatus.

Pressures in the gas-pressure vessels were read at the start of the runs on a precision Heise Bourdon tube gauge with an accuracy of $\pm 0.1\%$, and monitored throughout the runs on a manganin resistance cell previously calibrated against the Heise gauge. The maximum pressure uncertainty in the gas pressure vessels is ± 7 bars.

The temperature of the brucite-periclase equilibrium with pure H_2O at a nominal 4.2 kbar was found to be marginally lower in the gas-pressure experiments than in the piston-cylinder experiments ($718° \pm 3°$ C versus $723° \pm 3°$ C). This discrepancy, if real, could be the result of piston-cylinder pressure in the experiments near 4 kbar, which is actually 220 bars higher than the nominal pressure, or it could result from a real thermocouple calibration difference or a pressure effect on W-Re thermocouples in the piston-cylinder apparatus. Because of this uncertainty, the 4.2 kbar bracket is assigned an error of $\pm 5°$ C.

Detection of reaction

Reaction progress was detected by a weight loss method. After quenching an experiment, the Pt capsules were cleaned and reweighed to check for leakage. Weighings on a Mettler AE 240 semi-microbalance were reproducible to $\pm 2 \times 10^{-5}$ gm and showed no weight changes of the quenched capsules. The capsules were then immersed in liquid nitrogen to freeze the solution inside, and punctured with a needle while still frozen. The samples were removed from the liquid nitrogen and dried, first at 120° C for 10 min, and then at 320° C for 10 min. There was usually negligible additional weight loss in the second drying. A total drying loss greater than the weight of H_2O initially present in the capsule signified brucite decomposition; conversely a drying loss less than the initial H_2O indicated H_2O absorption by brucite growth. Reaction progress so monitored usually corresponded to nearly complete reactions in either direction. The reaction directions were confirmed by microscopic inspection of small portions of charges in immersion oil. Brucite was visible as large well-formed rounded or pseudohexagonal flakes, almost isotropic due to their planar orientation, but easily distinguishable from periclase by low relief, and as rectangular grains with very high birefringence, whereas periclase is isotropic and of very high index of refraction. This method by itself would have been sufficient to detect reaction directions unambiguously. Finally, the X-ray diffraction patterns of quenched charges were compared with those of the standardized starting mix. Again, nearly complete reactions were indicated by relative X-ray peak height changes in most of the runs.

Saturation of the salt solutions limits the concentrations of NaCl which could be obtained. Halite saturation was readily detected in two ways. The most definitive signal was inability to lower the brucite dehydration temperature beyond a certain limiting value in spite of increasing NaCl concentration of the charges, thus indicating that solutions were saturated. The second was the microscopic detection of large blocky halite crystals, interpreted as phenocrysts, among the skeletal arrays of melt-quenched salt and small inclusion-free salt grains precipitated on drying. A series of experiments was done specifically to define the saturation temperatures at a given pressure. The intersection of the isobaric brucite-periclase curve with the isobaric halite saturation curve in the system $MgO-H_2O-NaCl$ produces a temperature-invariant field boundary between brucite-halite-fluid and periclase-halite-fluid (see Fig. 3). Experiments at very high NaCl concentrations ($X_{H_2O}=0.2$ to 0.3) yielded reactions to either periclase or brucite over a 5° C interval enclosing this boundary, thus defining a point on the isobaric halite saturation curve.

Results of experiments

System $MgO-H_2O$

Figure 1 shows our brackets on the brucite-periclase equilibrium with pure H_2O to 15 kbar. The experimental data are presented in Table 1. All of the brackets constrain points on the equilibrium at 2, 4.2, 7, 10 and 15 kbar within an average of $\pm 4°$ C. Our determination agrees quite well with the unreversed 2 kbar bracket of Barnes and Ernst (1963). Franz's (1982) point (668°–673° C) at 2 kbar is several degrees higher than ours. His use of natural brucite starting material could possibly account for the discrepancy. The dynamic volumetric determinations of Schramke et al. (1982) at several pressures have wide temperature hysteresis; however, their heating-cycle signals coincide with the curve through our data. This may indicate delayed nucleation and growth of brucite in their cooling cycles. Near extrapolation to 15 kbar of the experimental brackets of Irving et al. (1977), obtained in the *P* range from 17 to 33 kbar, gives a temperature of 905° C, which agrees reasonably well with our determination (Table 1). The Berman (1988) and Holland and Powell (1990) thermodynamic datasets both yield 649° C at 2 kbar. Our use of coarse-grained periclase starting material, thus inhibiting back-reaction to brucite in the quench, removes some of the ambiguity from the determination.

The one-bar Gibbs free energy of the reaction is readily obtained by regression using the relation:

$$\Delta G^o(T,1) = -RTln f_{H_2O} - P\Delta V_s^* \quad (1)$$

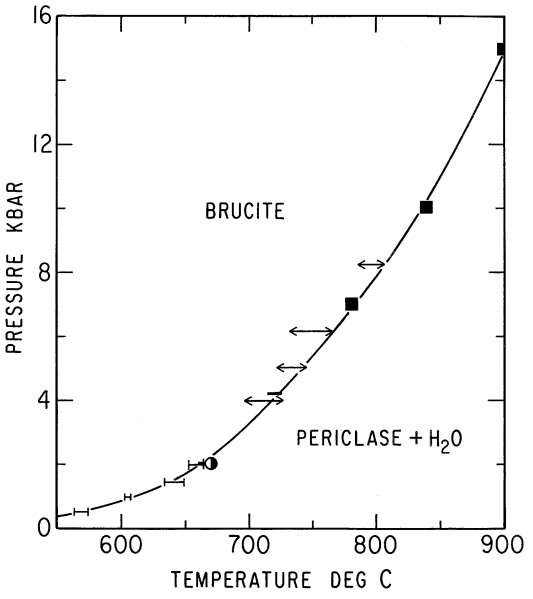

Fig. 1 Experimental brucite-periclase equilibrium in the system $MgO-H_2O$. Pressure and temperature uncertainties of present reversed determinations indicated by height and width of *filled rectangles*. Shown also are unreversed experimental brackets of Barnes and Ernst (1963) at 0.5 to 2 kbar, the hysteresis intervals (*double arrowheads*) determined by Schramke et al. (1982) in continuous volumetric reversals of the equilibrium, and the reversed bracket (*half-shaded circle*) at 2 kbar of Franz (1982)

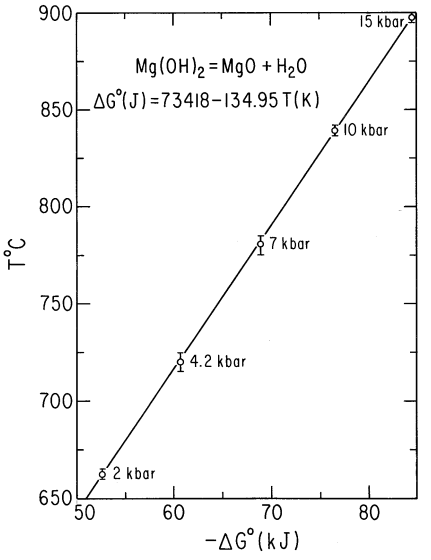

Fig. 2 Standard Gibbs free energy at one bar pressure for the reaction $Mg(OH)_2$ (brucite)=MgO (periclase)+H_2O, using the present experimental determinations, the H_2O fugacity tables of Burnham et al. (1969) extrapolated to 15 kbar with the help of the Sharp (1962) tables, and the compressibility and thermal expansion parameters for brucite and periclase of Holland and Powell (1990). The ΔG^o points are satisfied by the linear expression $\Delta G^o = 73418 - 134.95\ T(K)$, obtained by regression

Table 1 Experimental data on the reaction Br=Per+H_2O in pure water (*n/r* no to very little reaction progress detected by all methods)

Run #	*T*°C	*P*, kbar	Duration, h	Phase grown
PB-31	900	15.0	26	Per
PB-35	895	15.0	8	Br
PB-118	840	10.0	22	Per
PB-4	835	10.0	71	Br
PB-43	775	7.0	23	Br
PB-40	785	7.0	22	Per
PB-84	780	7.0	29	n/r
PB-98	725	4.2	46	Per
PB106	720	4.2	46	Br
PB-127[a]	720	4.2	44	Per
PB-129[a]	715	4.2	46	Br
PB-46[a]	660	2.0	69	Br
PB-62[a]	665	2.0	61	Per

[a] Runs made in the internally-heated gas apparatus; all the rest were piston-cylinder runs

where f_{H_2O} is the fugacity of H_2O at the experimental conditions and ΔV_s^* is the solid volume change, V(periclase)-V(brucite), evaluated at *T* and *P*/2. The above relation assumes that solubility of MgO is negligible and that the thermal expansion and compressibility coefficients are constants (volumes vary linearly with pressure and temperature). Our brackets together with H_2O fugacity data from Burnham et al. (1969) and thermal expansion and compressibility coefficients from Holland and Powell (1990) give the ΔG^o values shown in Fig. 2. They are satisfied within experimental uncertainties by the linear relation:

$$\Delta G^o\ (\pm 120J) = 73418 - 134.95\ T(K) \qquad (2)$$

Essentially the same relation is obtained employing thermophysical coefficients tabulated by Berman (1988).

System $MgO-H_2O-NaCl$

Figure 3 shows the brackets of brucite-periclase equilibrium in the system $MgO-H_2O-NaCl$ defined by initial and final fluid phase compositions. The complete dataset is given in Table 2. The closure of brackets at each temperature and pressure averages less than two mole percent width; many opposing reaction arrowheads are coincident. A very slight apparent cross-over was recorded in a few brackets. The brackets define unique isobaric univariant brucite-periclase-fluid equilibrium curves.

We were unable to secure brackets close to the pure H_2O axis. Experiments at 10 and 7 kbar and $X_{H_2O} > 0.93$ gave unexpected periclase-forming reactions, indicating that, in the very dilute range, the brucite-periclase equilibrium decreases in temperature more rapidly with increasing NaCl solution concentration than over most of the T–X_{H_2O} range (see Table 2). It is suspected that some solute complexing between MgO and NaCl occurs in dilute solutions, enhancing MgO solubility. The effect could be analogous to the augmented solubility of brucite in dilute K_2CO_3 solutions observed at low temperatures

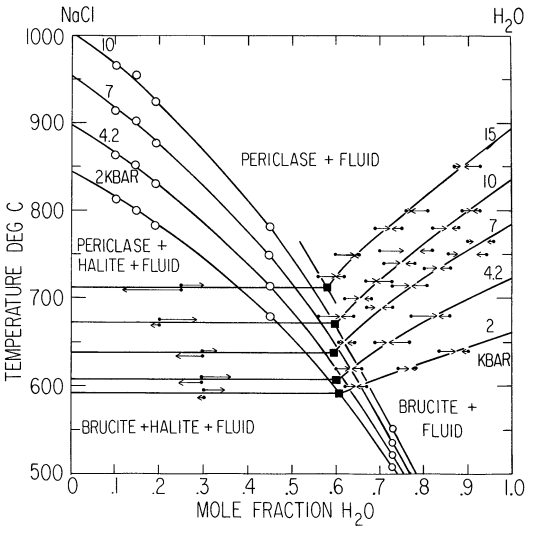

Fig. 3 Univariant and invariant equilibria in the system MgO−H_2O−NaCl at pressures of 2, 4.2, 7, 10 and 15 kbar. *Opposing arrows* show reversed equilibrated fluid compositions in equilibrium with brucite and periclase (*arrowheads*) starting from initial fluids indicated by the *dots* (*arrow tails*). The curves extend to our determinations in the system MgO−H_2O from Fig. 1. *Opposed arrows* at X_{H_2O}=0.2–0.3 show reversals of the isobaric invariant field boundary between brucite-halite-fluid and periclase-halite-fluid. Isobaric intersections of the univariant and invariant lines define five points on the halite saturation curves in the system NaCl−H_2O (*filled squares*) which are in good agreement with the family of curves determined by the DTA measurements to 6 kbar of Koster Van Groos (1991). Extrapolation of his data to 10 kbar incurs only small uncertainty. Melting points of pure NaCl at the five pressures are from Clark (1959) and Akella et al. (1969)

and pressures by Dernov-Pegarev et al. (1989). Higher concentrations of NaCl must destabilize any MgO−NaCl complexes, since experiments on the solubility of MgO at high NaCl concentrations, to be described, indicate vanishingly small solubilities. This would be the case if the postulated complexes were hydrated. Anomalous solubility in the dilute region may well be an important effect for some applications, but is not central to the present study, which focuses on concentrated solutions.

Brucite grown at a variety of P–T–X_{H_2O} conditions was analyzed for Cl with the electron microprobe. Comparison of some run products with starting material brucite as a standard showed detectable Cl in some products, up to a maximum of 0.17 wt%. Chlorine contents this small could not perturb the brucite-periclase equilibrium to any measurable extent.

The five sets of opposing arrows between X_{H_2O}=0.2 and 0.3 in Fig. 3 define temperature invariant phase boundaries which, by intersection with the isobaric brucite-periclase lines, in turn define points on the NaCl saturation curves. The saturation points at the five experimental pressures are indicated by filled squares. Also shown are points on the saturation curves determined, with minor interpolation and extrapolation, from the DTA experiments of Koster Van Groos (1991). It is seen that our saturation points agree very well with his data.

Table 2 Experimental data on the reaction Br=Per+H_2O in the presence of H_2O−NaCl solutions (*n/r* small change in water content in the course of the run, *Sat* runs under NaCl-saturated conditions)

Run #	*P*, kbar	*T*°C	Duration, h	X_{H_2O}, st.	X_{H_2O}, fin.	Phase grown
PB-49	15	850	9	0.870	0.881	Per
PB-50	15	850	9	0.930	0.893	Br
PB-41	15	800	20	0.760	0.771	Per
PB-42	15	800	20	0.810	0.775	Br
PB-53	15	780	24	0.690	0.723	Per
PB-54	15	780	24	0.750	0.728	Br
PB-44	15	750	8	0.685	0.677	Br-n/r
PB-45	15	750	8	0.740	0.683	Br
PB-48	15	750	20	0.646	0.635	n/r
PB-51	15	750	24	0.600	0.645	Per
PB-67	15	725	23	0.560	0.600	Per
PB-68	15	725	23	0.620	0.604	Br
PB-61	15	715	44	0.250	0.300	Per; sat.
PB-59	15	710	44	0.250	0.115	Br; sat.
PB-10	10	820	73	0.960	0.966	Per
PB-12	10	800	53	0.890	0.905	Per
PB-13	10	800	53	0.930	0.911	Br
PB-18	10	780	96	0.820	0.850	Per
PB-19	10	780	96	0.880	0.868	Br
PB-20	10	755	44	0.820	0.791	Br
PB-21	10	755	44	0.700	0.753	Per
PB-22	10	740	66	0.710	0.746	Per
PB-23	10	740	66	0.780	0.759	Br
PB-27	10	720	48	0.670	0.688	Per
PB-28	10	720	48	0.730	0.686	Br
PB-14	10	700	76	0.620	0.647	Per
PB-15	10	700	76	0.680	0.674	Br
PB-32	10	680	46	0.560	0.610	Per
PB-36	10	680	51	0.580	0.618	Per
PB-37	10	680	51	0.640	0.604	Br
PB-30	10	675	72	0.200	0.280	Per; sat.
PB-26	10	670	51	0.200	0.185	Br; sat.
PB-81	7	780	19	0.990	0.994	Per
PB-74	7	775	26	0.980	0.989	Per
PB-77	7	770	48	0.980	0.983	Per-n/r
PB-71	7	765	26	0.900	0.913	Per
PB-72	7	765	26	0.960	0.947	Br
PB-85	7	750	30	0.848	0.872	Per
PB-91	7	750	25	0.858	0.871	Per
PB-92	7	750	25	0.943	0.920	Br
PB-65	7	735	26	0.800	0.828	Per
PB-66	7	765	26	0.860	0.835	Br
PB-87	7	715	26	0.730	0.767	Per
PB-88	7	715	26	0.810	0.779	Br
PB-57	7	690	23	0.670	0.687	Per
PB-58	7	690	23	0.730	0.713	Br
PB-95	7	650	49	0.557	0.618	Per
PB-96	7	650	49	0.640	0.628	Br
PB-122	7	640	46	0.300	0.351	Per; sat.
PB-97	7	635	49	0.300	0.230	Br; sat.
PB-111	4.2	700	49	0.963	0.970	Per
PB-107	4.2	680	45	0.770	0.835	Per
PB-108	4.2	680	45	0.860	0.835	Br
PB-102	4.2	650	27	0.690	0.714	Per
PB-103	4.2	650	27	0.770	0.714	Br
PB-113	4.2	620	48	0.570	0.618	Per
PB-114	4.2	620	48	0.650	0.605	Br
PB-112	4.2	610	48	0.30	0.360	Per; sat.
PB-121	4.2	605	50	0.300	0.245	Br; sat.
PB-99	2	640	97	0.836	0.869	Per
PB-100	2	640	97	0.900	0.883	Br
PB-115	2	620	125	0.800	0.741	Br
PB-116	2	620	125	0.700	0.743	Per

Table 2 (continued)

Run #	*P*, kbar	*T*°C	Duration, h	X_{H_2O}, st.	X_{H_2O}, fin.	Phase grown
PB-104	2	600	141	0.623	0.652	Per
PB-105	2	600	141	0.702	0.635	Br
PB-126	2	590	96	0.300	0.292	Br; sat.
PB-130	2	595	99	0.300	0.346	Per; sat.

An extrapolation to 15 kbar of the DTA data would be too uncertain to provide a reliable comparison with our 15-kbar saturation point. Our 2 kbar saturation point is considerably different from that given by the DTA work of Gunter et al. (1983), who showed x_{H_2O}=0.53 at 600° C. The formulae of Sterner et al. (1992), based on the Gunter et al. (1983) work, give saturation curves to 5 kbar which are consistently less H_2O-rich than those found in the present study.

A few experiments were made to determine whether MgO solubility in concentrated NaCl solutions could have perturbed the halite saturation data or the H_2O activities derived below. Experiments were made with a very small amount of periclase (0.1 mg compared with the usual 2–4 mg of periclase+brucite in our normal experiments) and the normal amount of fluid. These solubility experiments were at 10 kbar and 700° C and X_{H_2O}=0.61, 0.67 and 0.76 for 48 h. In the experiment at X_{H_2O}=0.61, abundant large periclase crystals were present in the quenched charge, some showing geometrical overgrowths. No brucite formed. In the two experiments at higher H_2O concentration, abundant large geometrical brucite flakes formed, and occasional relics of periclase were visible in immersion oil, with reaction rims of brucite. These experiments show that the total contribution to the fluid phase of solute MgO must be much less than one mole percent. MgO solubilities this small could not measurably affect any of the phase equilibria or derived parameters in the system NaCl−H_2O.

Discussion

H_2O activity

H_2O activity a_{H_2O} in concentrated NaCl solutions can be derived accurately from measurements of the depression of the brucite-periclase equilibrium temperature, by use of the following expression:

$$RTlna_{H_2O} = -\Delta G^{o} - RTlnf_{H_2O} - P\Delta V_s^* \quad (3)$$

Fig. 4 shows the activity-concentration points derived from the experimental fluid-composition brackets of the periclase-brucite equilibrium. The uncertainties of the activity determinations are generally smaller than the sizes of the experimental symbols.

Our data confirm the deduction of Fanz (1982) that H_2O activities at 2 kbar in concentrated NaCl solutions

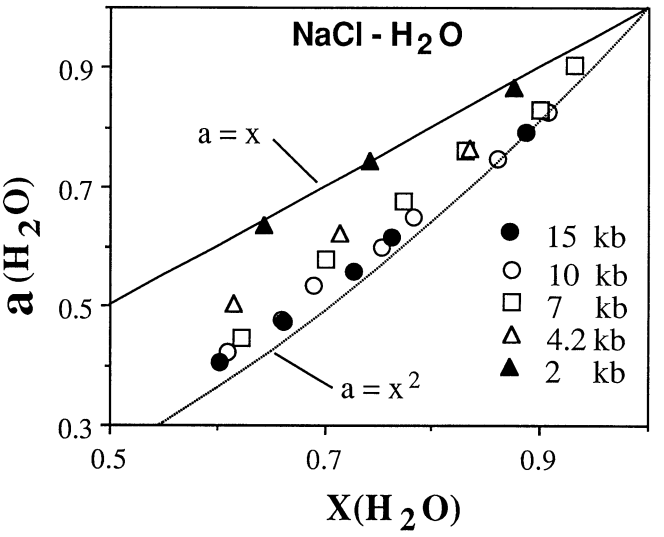

Fig. 4 Activity of H_2O (a_{H_2O}) as a function of H_2O mole fraction (X_{H_2O}) calculated from the brucite-periclase data of Fig. 3. Average uncertainties of the determinations are about the same sizes as the plotted symbols. At 2 kbar NaCl and H_2O are nearly ideal mixtures with H_2O activity equal to X_{H_2O}, but H_2O activity rapidly decreases below the mole fraction with increasing pressure, with values approaching the square of the mole fraction at 10–15 kbar. This trend is interpreted as resulting from pressure-induced dissociation of NaCl in the fluids (see text)

are nearly those expected of an ideal mixture of undissociated NaCl and H_2O; that is, the relationship $a_{H_2O}=X_{H_2O}$ is closely approximated. However, as pressure increases, a_{H_2O} becomes progressively smaller than X_{H_2O}, with an approach to the relationship $a_{H_2O}=X^2_{H_2O}$ at 15 kbar. The activity values at this pressure differ only slightly from those at 10 kbar. All of our derived H_2O activities fall in the sector between the curves for $a_{H_2O}=X_{H_2O}$ and $a_{H_2O}=X^2_{H_2O}$.

A simple interpretation of Fig. 4 is that the degree of dissociation of NaCl increases from nearly zero in the low-density range at 2 kbar to nearly complete dissociation above 10 kbar, where H_2O densities are near 1 gm/cm^3, or nearly the same as liquid water at standard conditions. This speculation is consistent with the accepted opinion that NaCl in aqueous solution exists mainly as the neutral complex at low pressures and higher temperatures (e.g. Walther 1992), but shows a strong tendency toward dissociation with increasing pressure (or density), as revealed by the conductance measurements of Quist and Marshall (1968). The present work is the first experimental evidence of a high degree of dissociation of solute NaCl in concentrated solutions at deep crustal and upper mantle pressure conditions.

NaCl activity

Our low degree of control of H_2O activity at low NaCl concentration rules out the possibility of obtaining NaCl activities by integrating the Gibbs-Duhem equation. However, individual NaCl activity values may be calcu-

lated in a straightforward manner from the five experimental saturation points, using the formula:

$$\int_{T_o}^{T_{sat}} \Delta S dT = RT_{sat} ln a_{NaCl} \quad (4)$$

where T_o is the halite melting point at P, T_{sat} is the temperature of our experimental saturation point at P, ΔS is the entropy of melting of pure NaCl and a_{NaCl} is the activity of NaCl in the hydrous liquid relative to a standard state of pure molten NaCl. ΔS is 26.22 J/K-mol at 1073 K and 1 bar, from Robie et al. (1978), and a small temperature correction to the entropy may be made using their heat capacity data:

$$\Delta C_p \text{ (melting)} = 26.857 - 0.0212\ T(K) \quad (5)$$

It is assumed that pressure up to several kbar has a negligible effect on ΔS of melting. This calculation yields the NaCl activity values from the five measured saturation points given in Table 3. The melting points of NaCl were taken from Clark's (1959) equation:

$$P \text{ (kbar)} = 16.7[(T/1073.5)^{2.70} - 1] \quad (6)$$

which reproduces very well the experimental data of Koster Van Groos (1991) and Akella et al. (1969) to 15 kbar.

Happenstantially, the five experimental saturation points are nearly invariant in composition, and close together in temperature, so that the effect of pressure on the activity coefficient of NaCl may be evaluated. The pressure effect is similar to that for H_2O: at 2 kbar the activity coefficient γ_{NaCl} is nearly unity, as it would be for an ideal binary solution, but pressure causes a substantial decrease at nearly constant composition, which probably results from pressure-induced ionization to Na^+ and Cl^-. The NaCl activities we calculate are somewhat larger than those given by the formulas of Sterner et al. (1992) because our saturation temperatures are higher than those given by these authors.

Thermodynamic model

The activity-concentration relationships for both H_2O and NaCl at 2 kbar are, to a close approximation, those of an ideal two-component mixture, where the activities are equal to their mole fractions (Table 4). In the intermediate and H_2O-rich composition ranges, this behavior corresponds to an ideal solution of H_2O molecules and undissociated NaCl molecules. It is not clear why the relationship persists to high NaCl concentration, inasmuch as fluids approaching pure molten NaCl in composition should presumably be completely ionized.

At 10 kbar the activities of both H_2O and NaCl are substantially smaller than their mole fractions, and, in fact, correspond closely to an ideal fused salt mixture in which the NaCl is completely ionized. The ideal (athermal) activities in this model, as developed by Bradley (1962) and by Pitzer and Simonson (1986) for NaCl−H_2O, are:

$$a^{id}_{H_2O} = X_{H_2O}/(2 - X_{H_2O}) \qquad a^{id}_{NaCl} = 4X^2_{NaCl}/(1 + X_{NaCl})^2 \quad (7)$$

The high degree of correspondence between the measured activities of both H_2O, from our brucite-periclase data, and NaCl, from our NaCl saturation points and the Koster Van Groos (1991) data, is shown in Table 4.

There thus appears to be a remarkable pressure/fluid density-induced change of state in NaCl- H_2O mixtures between 2 kbar and 10 kbar, which apparently results from dissociation of NaCl, and contributes a variable configurational entropy of solution. Extending the ideal activity formulation by Bradley (1962) and Pitzer and Simonson (1986) (Eq. 7 above), the following expressions can be readily obtained for the ideal activities of

Table 3 Activity (a) and activity coefficient (γ) of NaCl in the system NaCl−H_2O, calculated from the measured halite saturation data (ΔS^* is the mean value of entropy of melting of NaCl between T_0, the melting point at P in the H_2O-free system, and T_{sat}, the experimental halite saturation point in the system NaCl−H_2O at P)

P kbar	T_o K	T_{sat} K	ΔS^* J/K-mol	X_{NaCl}	a_{NaCl}	γ_{NaCl}
2.0	1117	866	25.82	0.395	0.406	1.09
4.2	1171	881	26.01	0.400	0.357	0.89
7.0	1221	911	26.19	0.405	0.342	0.85
10.0	1278	946	26.35	0.400	0.329	0.82
15.0	1361	986	26.50	0.420	0.298	0.71

Table 4 Comparison of measured and model activity values at 2.0 and 10.0 kbar

P (kbar)	T (°C)	X_{H_2O}	X_{NaCl}	$a^{meas}_{H_2O}$	$a^{id}_{H_2O}$	a^{meas}_{NaCl}	a^{id}_{NaCl}
2.0[a]	600	0.644		0.637	0.644		
	620	0.741		0.746	0.741		
	640	0.876		0.868	0.876		
	509		0.276			0.267	0.276
	593[c]		0.395[c]			0.407[c]	0.395[c]
	681		0.551			0.581	0.551
	782		0.812			0.824	0.812
	800		0.853			0.872	0.853
	813		0.900			0.907	0.900
10.0[b]	680	0.610		0.421	0.439		
	700	0.660		0.475	0.493		
	720	0.690		0.535	0.527		
	740	0.753		0.600	0.604		
	755	0.782		0.651	0.642		
	780	0.860		0.749	0.754		
	800	0.907		0.828	0.830		
	553		0.276			0.179	0.187
	673[c]		0.400[c]			0.329[c]	0.327[c]
	782		0.551			0.510	0.505
	923		0.812			0.803	0.803
	956		0.853			0.880	0.848
	968		0.900			0.909	0.898

[a] 2.0 kbar: $a^{id}_{H_2O} = X_{H_2O}$; $a^{id}_{NaCl} = X_{NaCl}$

[b] 10.0 kbar: $a^{id}_{H_2O} = X_{H_2O}/(2 - X_{H_2O})$; $a^{id}_{NaCl} = 4X^2_{NaCl}/(1 + X_{NaCl})^2$

[c] Our halite saturation measurements. Other a_{NaCl} data are calculated from the Koster Van Groos (1991) data, with minor interpolation and extrapolation (see text)

the components in solution with varying degree of ionization α:

$$a_{H_2O}=X_{H_2O}/(1+\alpha X_{NaCl})$$
$$a_{NaCl}=(1+\alpha)^{(1+\alpha)}[X_{NaCl}/(1+\alpha X_{NaCl})]^{(1+\alpha)} \quad (8)$$

α is a parameter, mainly dependent on pressure, temperature and fluid density, which is nearly zero at 2 kbar and nearly unity at 10 kbar and above. It may be viewed as a speciation parameter reflecting the number of the NaCl-related species in a solution relative to that in pure supercooled electrolite melt at any given pressure and temperature. It is evident that at $\alpha=1$, Eqs. 8 reduce to 7; at $\alpha=0$, Eqs. 8 give $a_{H_2O}=X_{H_2O}$ and $a_{NaCl}=X_{NaCl}$. The latter formulas correspond to another standard state widely used in thermodynamic modelling of the H_2O-NaCl system, that is, ideal molecular solution (e.g. Anderko and Pitzer 1993). It may also be readily verified that expressions 8 satisfy the Gibbs-Duhem relation if α is not a function of X_{H_2O}.

Several expressions for α as a function of *P, T* and water density (ϱ_{H_2O}) have been explored in the course of fitting the experimental data. Best results were obtained with the expression:

$$\alpha=\exp[A-B/\varrho_{H_2O}]-CP/T \quad (9)$$

This expression allowed for fitting of the 29 experimental fluid compositions measured in this study (24 points along the brucite-periclase equilibrium and 5 points on halite saturation) with standard deviation slightly below 0.010. For each particular point, the calculated fluid composition lies within the uncertainty of the experimental bracket. The resulting numerical values of the parameters of Eq. 9 are:

$$A=4.226, \quad B=2.9605, \quad C=164.984 \quad (10)$$

where *P* is in kbar, *T* in Kelvin, and ϱ_{H_2O} at the same *P* and *T* is in g/cm^3. The activity-composition relations computed with expressions 8 through 10 at 1000 K and different *P* values are shown in Fig. 5.

We can assess the validity of our formula outside the P–T–X_{H_2O} range of calibration by comparing calculated halite hydrous melting curves at 0.5, 2 and 5 kbar with experimental DTA determinations, shown in Fig. 6, by Gunter et al. (1983, as given in Table 2 of Chou et al. 1992) and Koster van Groos (1991). As can be seen, agreement between calculations and both experimental data sets at 0.5 kbar is very good. At $P=2$ kbar (the highest pressure of the Gunter et al. experiments) the computed melting curve lies between the two sets of measurements, and is somewhat closer to those by Koster van Groos (1991); at 5 kbar the agreement with the data by the latter author is also good, although the calculations predict melting temperatures which are systematically lower than the experimental temperatures by 5° to 10° C.

We also attempted to fit our data into the model suggested by Pitzer and Simonson (1986). This model, which represents a combination of the Debye-Hückel limiting equation with a Margules power series to account for short-range electrostatic forces in solution, proved to reproduce very well water activity measurements in dilute to concentrated electrolyte solutions (Simonson and Pitzer 1986; Weres and Tsao 1986). The model, however, failed to reproduce simultaneously the H_2O and the NaCl activity values obtained in this study, even when we allowed the W parameter to be linearly dependent on both *P* and *T*. The extension of the model proposed by Pabalan and Pitzer (1990) relies upon too many parameters to be evaluated with the data of the present study.

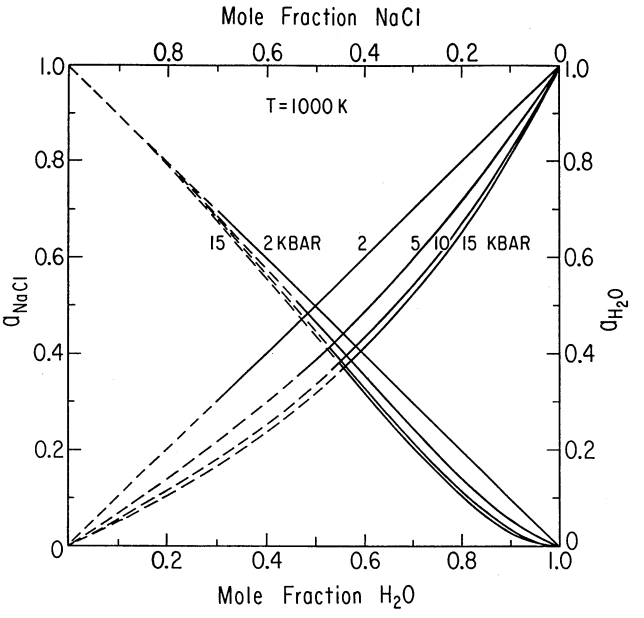

Fig. 5 Activity-composition relations of H_2O and NaCl in the binary join evaluated from the simple ideal expressions of the text. The curves are *dashed* in their metastable portions beyond the halite saturation points at 1000 K

It is apparent that activity-composition relations of the system NaCl−H_2O at high *T, P* and X_{NaCl} are much simpler than inferred by the extended Debye-Hückel formulation; in fact the solutions behave as nearly ideal mixtures of ions and molecules in which the degree of NaCl ionization is a strong function of pressure and temperature (dielectric constant/density of water) in the range 2–10 kbar. It is also apparent that the molten NaCl standard state is much preferable in simple modelling of the thermodynamics than the dilute solution standard state. We should point out, however, that although the parameter α, as it appears in this study, is closely analogous to the traditional degree of dissociation (e.g. Quist and Marshall 1968), it differs from the latter in two important respects: first, it does not depend on the concentration of electrolyte in a solution, and second, under certain values of *P, T*, and ϱ_{H_2O} it can become slightly negative, or greater than 1, which reflects more complex solution behavior of NaCl (e.g. hydration and/or dissociation of H_2O, as well as deviation of the NaCl−H_2O system from ideality).

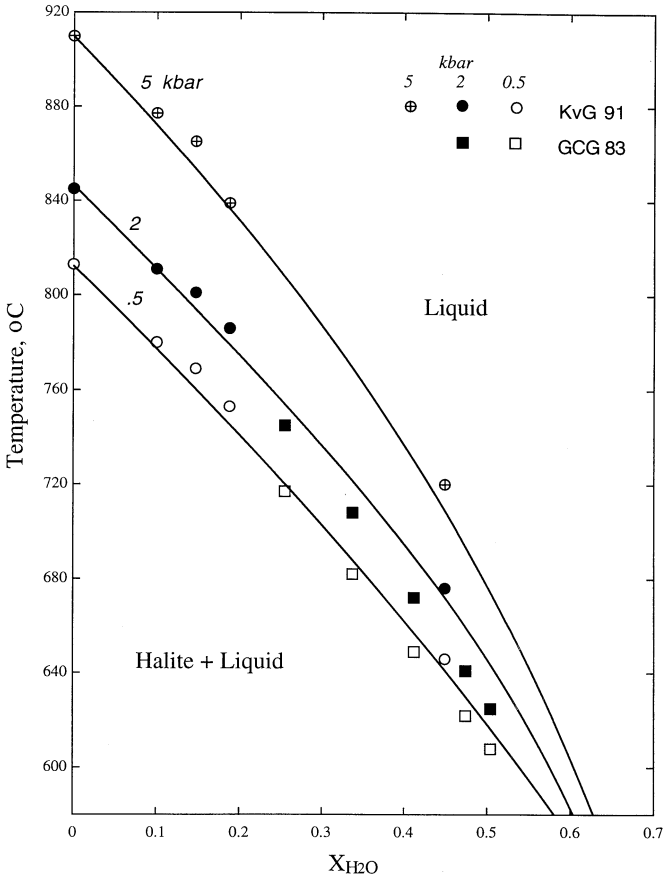

Fig. 6 Temperature (T°)-mole fraction of water (X_{H_2O}) isobars (*labelled curves*) of the halite liquidus calculated from the "ideal activity" model (see text) compared with experimental DTA measurements by Koster van Groos (KvG 1991; *circles*) and Gunter et al. (GCG 1983; *squares*)

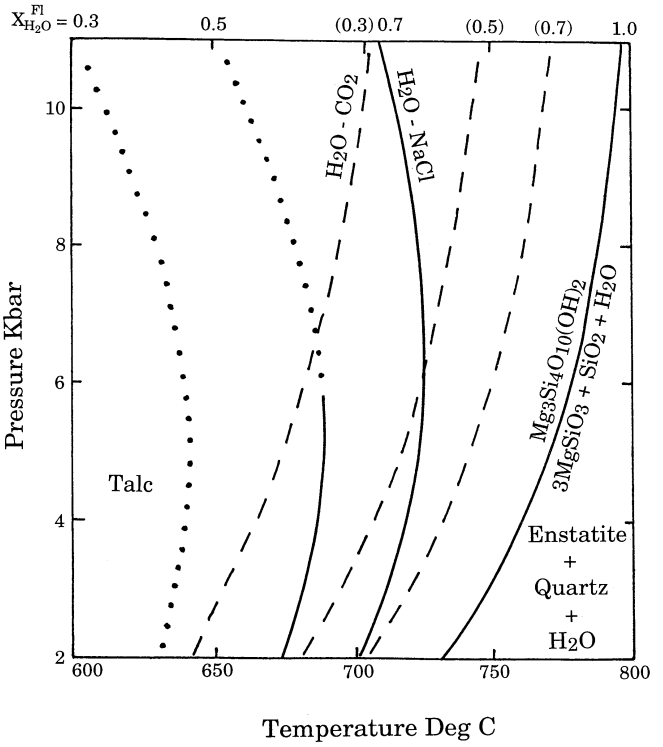

Fig. 7 Calculated P–T projections of the equilibrium talc-enstatite+quartz+H_2O at various compositions of the fluid phase (X_{H_2O} labelled at the top of diagram) in the systems $H_2O-NaCl$ (*bold curves; dotted* at NaCl concentrations above saturation) and H_2O-CO_2 (*dashed*)

Petrologic interpretations

A principal requisite of fluids which are feasible for deep crust and upper mantle metamorphism is low H_2O activity, while maintaining the ability to exchange alkalis, as in charnockitic metamorphism (Perchuk and Gerya 1993) and in mantle metasomatism (Dawson and Smith 1992). Halogen zoning patterns in apatite from the Bamble, S. Norway granulites (Nijland et al. 1993) show attack by deep crustal fluids which were probably concentrated brines. Our results show that $NaCl-H_2O$ solutions may have H_2O activities as low as 0.25 at 750° C and 10 kbar; this would be sufficiently low to be in equilibrium with orthopyroxene and K-feldspar, the definitive granulite assemblage, while allowing only limited, rather than wholesale, crustal anatexis.

In all probability, natural concentrated brines would contain a variety of other cations, such as Ca^{2+}, Mg^{2+}, Fe^{2+}, Fe^{3+} and K^+, and other anions, such as CO_3^{2-} SO_4^{2-}, F^-, etc. For instance, DeJong and Williams (1995) inferred $CaCl_2$/NaCl of about 2 (wt ratio) from melting behavior of salt crystal-brine inclusions in metasomatized rocks of the Cloncurry Fault area, Queensland. The presence of complex electrolytes would further lower H_2O activity at a given H_2O mole fraction, if pressure-induced ionization is indeed a principal control, and, perhaps more importantly, these additional salts would form a low-melting eutectic with NaCl, thus further lowering the temperatures of the saturation curves, allowing higher salt concentrations and hence lower H_2O activities.

The effect of concentrated NaCl solutions on the upper temperature stability limit of hydrous silicates is illustrated in Fig. 7. A simple and well known high-temperature dehydration reaction occurs in the system $MgO-SiO_2-H_2O$:

Talc=Enstatite+Quartz+H_2O.

The equilibrium P–T position of this reaction at X_{H_2O} =1.0 and in H_2O-CO_2 mixes with fixed X_{H_2O} was calculated employing the mineral thermodynamic data set of Berman and Aranovich (1996) and H_2O-CO_2 mixing properties according to Kerrick and Jacobs (1981). Expressions 8–10 have been used to calculate the position of the reaction in the presence of $H_2O-NaCl$ fluid.

At low pressure (up to ~4 kbar) dehydration temperatures of talc for a given X_{H_2O} do not differ much in H_2O-CO_2 and $H_2O-NaCl$, but the difference becomes much greater with increasing P (up to 70° C difference at 10 kbar), which is a direct consequence of the extremely pressure-dependent H_2O activity in the $H_2O-NaCl$ sys-

tem found in this study. It is also important that the dP/dT slope of the dehydration reaction in the salt-bearing system changes its sign from positive to negative, in contrast with that in the H_2O-CO_2, where it remains positive, at least in the crustal pressure range. The above example shows that concentrated brines are much more efficient in stabilizing anhydrous assemblages to lower temperatures than H_2O-CO_2 fluids, thus satisfying one important requisite of the fluid agent of granulite facies metamorphism.

Another requisite of possible granulite-facies fluids is that extensive melting be suppressed at the high temperatures and pressures of deep crustal metamorphism. The pronounced decrease of H_2O activity in concentrated NaCl solutions at pressures above a few kbar suggests that such fluids might indeed be able to coexist with feldspars and quartz without melting at high grade conditions.

The problem of deep crustal melting in the presence of concentrated alkali chloride solutions may be approached quantitatively making use of experimental simple-system granite melting relations with CO_2-H_2O fluids (Ebadi and Johannes 1991). Increasing CO_2 in the vapor phase substantially raises the solidus in the system $KAlSi_3O_8$ (Or)$-NaAlSi_3O_8$ (Ab)$-SiO_2$ (Qz)$-H_2O$. Comparison of the relative effects of the solutes CO_2 and NaCl on granite melting may be made with the present experimental work and the Ebadi and Johannes (1991) data, together with experimental data of alkali partitioning between coexisting K-feldspar and albite, and chloride solutions. According to Iiyama (1965), the Na/Na+K ratio of relatively dilute solutions in equilibrium with two feldspars at 600° C and one kbar is very high (0.8), and it is assumed here that chloride solutions at the granite solidus remain Na-dominated at higher temperatures, pressures and concentrations. This assumption allows use of the present $H_2O-NaCl$ activity-concentration relations for solutions containing a subsidiary amount of KCl in addition to NaCl. Since the granite solidus is determined principally by a_{H_2O} at a given T and P, the Ebadi and Johannes (1991) solidus curves for fixed H_2O mole fraction in CO_2-H_2O fluids determine corresponding solidus curves in $NaCl-H_2O$ fluids. It is further assumed that the minimum melt compositions in the presence of chloride fluids are not greatly different from those under CO_2-H_2O fluids. Experiments (Metrich and Rutherford 1992; Shinohara et al. 1989) show that the chlorine content of brine-saturated silicate melts is negligible above 2 kbar. The $a_{H_2O}-X_{H_2O}$ relations used by Ebadi and Johannes (1991), based on the Redlich-Kwong equation of state, are adopted here, along with equations 8–10 of the present work, leading to the granite solidus curves shown in Fig. 8.

The notable changes in dP/dT slopes of the solidus curves above two kbar are a predictable result of the great decrease of H_2O activity in NaCl solutions at higher pressures. This behavior contrasts with that of the CO_2-H_2O system, where H_2O activity rises with increasing pressure at a given composition and temperature. Consequently, for a fluid of 50 mole percent H_2O, the $NaCl-H_2O$ melting curve at 10 kbar lies 105° C higher than the corresponding CO_2-H_2O melting curve. Melting curves of the two systems converge below 2 kbar as ideal solution behavior is approached in both fluid systems.

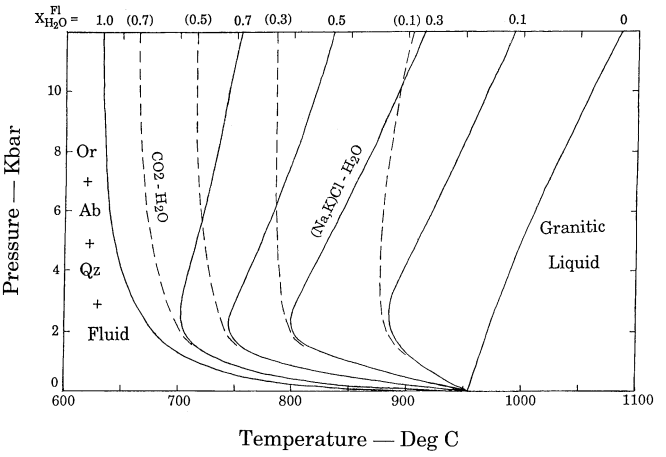

Fig. 8 Solidus curves in the simple granite system $KAlSi_3O_8$ (Or)$-NaAlSi_3O_8$ (Ab)$-SiO_2$ (Qz)$-H_2O$ for NaCl solutions of fixed X_{H_2O}, calculated from the present activity-concentration relations in the $NaCl-H_2O$ system, and corresponding X_{H_2O} curves in the system CO_2-H_2O (*dashed*), from Ebadi and Johannes (1991)

An important consequence for petrology of the backbending brine-granulite solidi is that concentrated chloride solutions may stream freely through the lower crust at elevated temperatures without provoking extensive melting, and can have H_2O activity low enough to destabilize hydrous silicate minerals including biotite and amphibole, while retaining the ability to exchange alkalis as well as volatiles, in keeping with the concept of the alkalis as mobile components in metamorphism (Korzhinskii 1959). In all of these regards, the brines are conceptually superior to CO_2-H_2O solutions which, at equivalent H_2O mole fractions, have higher H_2O activity, lower granite solidi, and greatly reduced solubilities of the silicate constituents (Holloway 1971; Walther 1992). Moreover, aqueous salt solutions make very small contact angles with silicate minerals in rocks at high temperatures and pressures and therefore have much greater infiltration ability than CO_2-rich fluids, which make high contact angles with silicate minerals (Watson and Brenan 1987).

Acknowledgements This research was supported by a U.S. National Science Foundation grant, #EAR-9310264. The authors acknowledge helpful conversations and correspondence with Lucas Baumgartner, Bill Glassley, Kirill Shmulovich, Jacques Touret, Volkmar Trommsdorff, Paul Wallace, John Walther, and Pat Williams. Constructive comments on the first draft of the manuscript by Bill Glassley and Tim Holland are also greatly appreciated.

References

Akella J, Vaidya SN, Kennedy GC (1969) Melting of sodium chloride at pressures to 65 kbar. Phys Rev 185: 1135–1140

Anderko A, Pitzer KS (1993) Equation-of-state representation of phase equilibria and volumetric properties of the system NaCl−H_2O above 573 K. Geochim Cosmochim Acta 57: 1657–1680

Aranovich LYa, Shmulovich KI, Fedkin VV (1987) The H_2O and CO_2 regime in regional metamorphism. Int Geol Rev 29: 1379–1401

Barnes HL, Ernst WG (1963) Ideality and ionization in hydrothermal fluids: the system MgO−H_2O−NaOH. Am J Sci 261: 129–150

Berman RG (1988) Internally-consistent thermodynamic data for minerals in the system Na_2O−K_2O−CaO−MgO−FeO−Fe_2O_3−Al_2O_3−SiO_2−TiO_2−H_2O−CO_2. J Petrol 29: 445–522

Berman RG, Aranovich LY (1996) Optimized standard state and solution properties of minerals: I. Model calibration for olivine, orthopyroxene, cordierite, garnet, and ilmenite in the system FeO−MgO−CaO−Al_2O_3−TiO_2−SiO_2. Contrib Mineral Petrol (in press)

Bowers TS, Helgeson HC (1983) Calculation of the thermodynamic and geochemical consequences of nonideal mixing in the system H_2O−CO_2−NaCl on phase relations in geologic systems: equation of state of H_2O−CO_2−NaCl fluids at high pressures and temperatures. Geochim Cosmochim Acta 47: 1247–1275

Bradley RS (1962) Thermodynamic calculations on phase equilibria involving fused salts. Part I. General theory and application to equilibria involving calcium carbonate at high pressure. Am J Sci 260: 374–382

Burnham CW, Holloway JR, Davis NF (1969) Thermodynamic properties of water to 1000° C and 10 000 bars. Geol Soc Am Spec Pap 132

Chou I-M, Sterner SM, Pitzer KS (1992) Phase relations in the system NaCl−KCl−H_2O: IV. Differential thermal analysis of the sylvite liquidus in the KCl−H_2O binary, the liquidus in the NaCl−KCl−H_2O ternary, and the solidus in the NaCl−KCl binary to 2 kb pressure, and a summary of experimental data for thermodynamic-PTX analysis of solid-liquid equilibria at elevated P–T conditions. Geochim Cosmochim Acta 56: 2281–2293

Clark SP Jr (1959) Effect of pressure on the melting point of eight alkali halides. J Chem Phys 31: 1526–1531

Dawson JB, Smith JV (1992) Potassium loss during metasomatic alteration of mica pyroxenite from Oldoinyo Lengai, northern Tanzania: contrasts with fenitization. Contrib Mineral Petrol 112: 254–260

DeJong G, Williams PJ (1995) Giant metasomatic system formed during exhumation of mid-crustal Proterozoic rocks in the vicinity of the Cloncurry Fault, northern Queensland. Aust J Earth Sci 42: 281–290

Dernov-Pegarev VF, Bogomolova VI, Malinin SD (1989) The solubility of brucite and forsterite in K_2CO_3 and Na_2CO_3 solutions at 300 and 400° C as it relates to carbonatite formation. Geochem Int 26: 68–73

Ebadi A, Johannes W (1991) Beginning of melting and composition of first melts in the system Qz−Ab−Or−H_2O−CO_2. Contrib Mineral Petrol 106: 286–295

Franz G (1982) The brucite-periclase equilibrium at reduced H_2O activities: some information about the system H_2O−NaCl. Am J Sci 282: 1325–1339

Graton LC (1940) Nature of the ore-forming fluids. Econ Geol 35: 197–358

Gunter WD, Chou I-M, Girsperger S (1983) Phase relations in the system NaCl−KCl−H_2O: differential thermal analysis of the halite liquidus in NaCl−H_2O binary above 450° C. Geochim Cosmochim Acta 47: 863–873

Holland TJB, Powell R (1990) An enlarged and updated internally consistent thermodynamic dataset with uncertainties and correlations: the system K_2O−Na_2O−CaO−MgO−MnO−FeO−Fe_2O_3−Al_2O_3−TiO_2−SiO_2−C−H_2−O_2. J Metamorphic Geol 8: 89–124

Holloway JR (1971) Composition of fluid phase solutes in a basalt-H_2O−CO_2 system. Geol Soc Am Bull 62: 233–238

Iiyama JT (1965) Influence des anions sur les équilibres d'échange d'ions Na–K dans les feldspaths alcalins à 600° C sous une pression de 1000 bars. Bull Soc Fr Minéral Cristalogr 88: 618–622

Irving AJ, Huang W-L, Wyllie PJ (1977) Phase relations of portlandite, $Ca(OH)_2$ and brucite, $Mg(OH)_2$ to 33 kilobars. Amer J Sci 277: 313–321

Johannes W, Metz P (1968) Experimentelle Bestimmung von Gleichgewichtsbeziehungen im System MgO−CO_2−H_2O. Neues Jahrb Mineral Abh 112: 15–26

Keevil NB (1942) Vapor pressure of aqueous solutions at high temperatures. J Am Chem Soc 64: 841–850

Kerrick DM, Jacobs GK (1981) A modified Redlich-Kwong equation for H_2O, CO_2, and H_2O−CO_2 mixtures at elevated pressures and temperatures. Am J Sci 281: 735–767

Korzhinskii DS (1959) Physiochemical basis of the analysis of the paragenesis of minerals. Consultants Bureau, New York

Koster Van Groos AF (1991) Differential thermal analysis of the liquidus relations in the system NaCl−H_2O to 6 kbar. Geochim Cosmochim Acta 55: 2811–2817

Lowenstern JB (1994) Chlorine, fluid immiscibility, and degassing in peralkaline magmas from Pantelleria, Italy. Am Mineral 79: 353–369

Marakushev AA, Shapovalov YuB (1994) Main problems of origin of hydrothermal ore deposits (experimental investigations). Exp Geosci 3: 1–10

Metrich N, Rutherford MJ (1992) Experimental study of chlorine behavior in hydrous silicic melts. Geochim Cosmochim Acta 56: 607–616

Nijland TG, Jansen JBH, Maijer C (1993) Halogen geochemistry of fluid during amphibolite-granulite metamorphism as indicated by apatite and hydrous silicates in basic rocks from the Bamble Sector, South Norway, Lithos 30: 167–189

Oliver NHS (1995) Hydrothermal history of the Mary Kathleen Fold Belt, Mt. Isa Block, Queensland. Aust J Earth Sci 42: 267–279

Pabalan RT, Pitzer KS (1990) Models for aqueous electrolyte mixtures for systems extending from dilute solutions to fused salts. In: Melchior DC, Bassett RL (eds) Chemical Modeling of Aqueous Systems II, (American Chemical Society Series 416). American Chemical Society, Washington DC, pp 44–57

Pasteris JD, Harris TN, Sassari DC (1995) Interactions of mixed volatile-brine fluids in rocks of the southwestern footwall of the Duluth Complex, Minnesota – evidence from aqueous fluid inclusions. Am J Sci 295: 125–172

Perchuk LL, Gerya TV (1993) Fluid control of charnockitization. Chem Geol 108: 175–186

Philipp RW (1988) Phasenbeziehungen im system MgO−H_2O−CO_2−NaCl. Dipl Natur thesis, ETH-Zürich

Philippot P, Selverstone J (1991) Trace-element-rich brines in eclogitic veins: implications for fluid composition and transport during subduction. Contrib Mineral Petrol 106: 417–430

Pitzer KS, Simonson JM (1986) Thermodynamics of multicomponent, miscible ionic systems: theory and equations. J Phys Chem 90: 3005–3009

Quist AS, Marshall WL (1968) Electrical conductances of aqueous sodium chloride solutions from 0 to 800° C and at pressures up to 4000 bars. J Phys Chem 72: 684–703

Robie RA, Hemingway BS, Fisher JR (1978) Thermodynamic properties of minerals and related substances at 298.15° K and 1 bar (105 pascals) pressure and at higher temperatures. US Geol Surv Bull 1452: 1–456

Roedder E (1971) Fluid inclusion studies on porphyry-type ore deposits at Bingham, Utah, Butte, Montana, and Climax, Colorado. Econ Geol 66: 98–120

Samson IM, Liu W, Williams-Jones AE (1995) The nature of orthomagmatic fluids in the Oka carbonatite, Quebec, Canada: evidence from fluid inclusions. Geochim Cosmochim Acta 59: 1963–1977

Schranke JA, Kerrick DM, Blencoe JG (1982) Experimental determination of the brucite-periclase equilibrium with a new volumetric technique. Am Mineral 67: 269–276

Sciuto PF, Ottonello G 81995) Water-rock interaction on Zabargad Island, Red Sea – a case study: I. Application of the concept of local equilibrium. Geochim Cosmochim Acta 59: 2187–2206

Sharp WE (1962) The thermodynamic functions for water in range −10 to 1000° C and 1 to 250 000 bars. University of California, Ernest O. Lawrence Radiation Laboratory Publication UCRL-718 (Chemistry, UC-4)

Shinohara H, Iiyama JT, Matsuo S (1989) Partition of chlorine compounds between silicate melt and hydrothermal solutions. II. Partition of $NaCl-H_2O$. Geochim Cosmomich Acta 53: 2617–2630

Shmulovich KI (1988) Carbon dioxide in high-temperature processes of mineral formation (in Russian). Nauka Press, Moscow

Shmulovich KI, Shmonov VM, Zharikov VA (1982) The thermodynamics of supercritical fluid systems. In: Saxena SK (eds) Advances in physical geochemistry. Springer, Berlin Heidelberg New York, pp 173–190

Shmulovich KI, Tkachenko SI, Plyasunova NV (1995) Phase equilibria in fluid systems at high pressures and temperatures. In: Shmulovich KI, Yardley BWD, Gonchar GG (eds) Fluids in the Crust. Chapman and Hall, London, pp 193–214

Simonson JM, Pitzer KS (1986) Thermodynamics of multicomponent, miscible, ionic systems: the system $LiNO_3-KNO_3-H_2O$. J Phys Chem 90: 3009–3013

Smith FG (1948) Transport and deposition of the non-sulphide vein minerals. III. Phase relations at the pegmatitic stage. Econ Geol 43: 535–546

Sourirajan S, Kennedy GC (1962) The system $H_2O-NaCl$ at elevated temperatures and pressures. Am J Sci 260: 115–141

Sterner SM, Chou I-M, Downs RT, Pitzer KS (1992) Phase relations in the system $NaCl-KCl-H_2O$: V. Thermodynamic-PTX analysis of solid-liquid equilibria at high temperatures and pressures. Geochim Cosmochim Acta 56: 2295–2309

Touret JLR (1985) Fluid regime in southern Norway: the record of fluid inclusions. In: Tobi AC, Touret JRL (eds) The deep Proterozoic crust in the North Atlantic provinces. Reidel, Dordrecht, pp 517–549

Touret JRL (1995) Brines in granulites: the other fluid. (abstract). ECROFI (European Conference on Fluid Inclusions), Barcelona, June 1995

Walther JV (1992) Ionic association in H_2O-CO_2 fluids at mid-crustal conditions. J Metamorphic Geol 10: 789–797

Watson ED, Brenan JM (1987) Fluids in the lithosphere, 1. Experimentally-determined wetting characteristics of CO_2-H_2O fluids and their implications for fluid transport, host-rock physical properties, and fluid inclusion formation. Earth Planet Sci Lett 85: 497–515

Weres O, Tsao L (1986) Activity of water mixed with molten salts at 317° C. J Phys Chem 90: 3014–3018